LHC discovery potential of the lightest NMSSM Higgs in $h \to a_1 a_1 \to \mu\mu\mu\mu$ channel

Alexander Belyaev,[1,2] Jim Pivarski,[3] Alexei Safonov,[3] and Sergey Senkin[3]

[1] School of Physics & Astronomy, University of Southampton,
Highfield, Southampton SO17 1BJ, UK
[2] Particle Physics Department, Rutherford Appleton Laboratory,
Chilton, Didcot, Oxon OX11 0QX, UK
[3] Physics Department, Texas A&M University
(Dated: November 25, 2009)

We explore the potential of Large Hadron Collider to observe $h_1 \to a_1 a_1 \to 4\mu$ signal from the lightest lightest scalar Higgs boson (h_1) decaying into two lightest pseudoscalar Higgs bosons(a_1) followed by their decays into 4 muons within the Next-to-Minimal Supersymmetric Standard Model (NMSSM). The signature under study allows to cover the NMSSM parameter space with M_{a_1} below 3.5 GeV and large $Br(h_1 \to a_1 a_1)$ which has not been studied previously. In case of such a scenario, the suggested strategy of the observation of 4μ signal with the respective background suppression would provide a unique way to discover the lightest scalar NMSSM Higgs boson.

INTRODUCTION

The next-to-minimal supersymmetric standard model (NMSSM) [1–13] is extended by one singlet superfield in addition to the particle content of the Minimal Supersymmetric Standard Model (MSSM). NMSSM has several new attractive features as compared to MSSM. First of all, NMSSM elegantly solves so called μ-problem [14]: the scale of the μ-parameter is automatically generated at the electroweak or SUSY scale when the singlet Higgs acquires a vacuum expectation value. On the other hand NMSSM can solve fine-tuning and little hierarchy problems of MSSM [15]. The upper mass limit on the lightest CP-even Higgs boson in NMSSM is larger than in MSSM and since more parameter space survives LEP II bounds from the Higgs search, NMSSM is less fine-tuned. On the other hand there is additional mechanism for the reduction of fine-tuning since LEP II bounds from the Higgs search can be partly avoided if the branching of $h_1 \to a_1 a_1$ decay is significant (h_1 and a_1 stands for the lightest CP-even and CP-odd Higgs bosons respectively). This decay channel of h_1 diminishes the branching ratios for conventional modes used in direct Higgs searches and largely softens direct Higgs boson mass limits from LEP.

One should stress that due to the extended scalar sector (in comparison to MSSM) NMSSM offers richer Higgs collider phenomenology [16–24] as well as richer cosmological Dark Matter implications related to the presence of the fifth neutralino ("singlino"), relic density for which can be achieved to be correct one [25].

The collider phenomenology of the Higgs sector of the NMSSM is very interesting in several aspects, therefore a short historical introduction is in order. In [17] the first attempt to establish 'no-lose' theorem for NMSSM has been done. This theorem states that LHC has a potential to discover at least one NMSSM Higgs boson in the conventional mode given that Higgs-to-Higgs decay modes are not important. However the point is that Higgs-to-Higgs decay modes can be important as has been shown and studied later on in analysis devoted to re-establishing of 'no-lose' theorem [18–24] for the case when $h_1 \to a_1 a_1$ decay is significant and a_1 is light. So far, the case of the lightest a_1 was explored for m_{a_1} below $2b$-quark threshold but above 2τ one, $2m_\tau < m_{a_1} < 2m_b$, establishing the scope of the 4τ channel in Higgs-strahlung and Vector Boson Fusion for the NMSSM No-Lose Theorem at the LHC [24]. Theses analysis require a substantial integrated luminosity (10-100 fb^{-1}) and quite challenging analysis in the technical sense.

In this paper we explore the mass region of a_1 with the mass below 2τ threshold: $m_{a_1} < 2m_\tau$. In this case, which has not been studied previously, we explore the potential of $h_1 \to a_1 a_1 \to \mu\mu\mu\mu$ signature at the LHC. Unlike searches for 4τ signature, the measurement of invariant mass of muon pair provides a direct estimate of m_{a_1} which defines a clear set of the kinematical cuts for the background suppression. Further, this channel is essentially free of backgrounds and therefore allows to use direct gluon fusion production combined with $b\bar{b}$ fusion production instead of subdominant vector boson fusion or associate Higgs production processes used in case of 4τ signature to to suppress large QCD backgrounds.

We demonstrate that the analysis in the four muon mode has excellent sensitivity for Lightest CP-even NMSSM Higgs boson and can be performed with just a handful of first LHC data and requires very little in terms of detector performance except reasonably robust tracking for muons and well functioning muon system. To make this a realistic analysis, we use parameters of the CMS experiment in designing selections and estimating background contributions.

The rest of the paper is organized as follows. In Section II we study the NMSSM parameters space for which $m_{a_1} < 2m_\mu$ case of our study is realized. In Section III we perform signal versus background analysis and present our final results in Section IV. In Section V we draw our conclusions.

NMSSM PARAMETER SPACE

In our study we consider the simplest version of the NMSSM [1–12], in which the $\mu \widehat{H}_1 \widehat{H}_2$ term of the MSSM superpotential is replaced by

$$\lambda \widehat{S}\widehat{H}_1\widehat{H}_2 + \frac{\kappa}{3}\widehat{S}^3, \tag{1}$$

which makes the superpotential scale invariant. In general, we have five soft braking terms; in the "non-universal" case,

$$m^2_{H_1}H_1^2 + m^2_{H_2}H_2^2 + m^2_S S^2 + \lambda A_\lambda H_1 H_2 S + \frac{\kappa}{3}A_\kappa S^3. \tag{2}$$

In the above equations, capital letters with tildes denote superfields while symbols without tildes denote the scalar component of the respective superfield.

Soft breaking parameters $m^2_{H_1}$, $m^2_{H_2}$ and m^2_S from Eq.(2) can be replaced by M_Z, the ratio of the doublet Higgs vacuum expectation values (VEVs) $\tan\beta$, and $\mu = \lambda\langle S\rangle$ (where $\langle S\rangle$ denotes the VEV of the singlet Higgs field) through the three minimization equations of the Higgs potential. Assuming that the Higgs sector is CP conserving, the NMSSM Higgs sector at the Electro-Weak (EW) scale is uniquely defined by 14 parameters: $\tan\beta$, the trilinear couplings in the superpotential λ and κ, the corresponding soft SUSY breaking parameters A_λ and A_κ, the effective μ parameter $\mu = \lambda\langle S\rangle$, the gaugino mass parameters M_1, M_2 and M_3, the squark and slepton trilinear couplings A_t, A_b and A_τ, and the squark and slepton mass parameters M_{f_L} and M_{f_R}. For simplicity, we assume here the universality within 3 generations for the last two parameters, leaving only 6 parameters for sfermion masses.

Phenomenology of the low-m_a region of the NMSSM

To find the parameter space for our region of interest, $m_a < 2m_\tau$, we scan the NMSSM parameter space using the NMSSMTools package [26–28], applying all known phenomenological and experimental constraints except the following: the cosmological dark matter relic density measured by WMAP [29], direct $p\bar{p}{\to}h_1{\to}aa{\to}4\mu$ and 2μ, 2τ searches by the Tevatron [30], direct $e^+e^-{\to}Zh_1$, $h_1{\to}aa$ searches by LEP [31, 32], and direct $\Upsilon{\to}\gamma a$ searches by CLEO [33] and BaBar [34]. These important constraints will be applied explicitly to our region of interest in a later section.

We scanned the NMSSM parameter space uniformly in the following:

- 100 GeV $< \mu < 1000$ GeV
- $0 < \lambda < 1$
- $1.5 < \tan\beta < 50$

- -1 TeV $< A_\lambda < 5$ TeV
- $0 < \mu\kappa/\lambda < 120$ GeV
- -3 GeV $< A_\kappa - (30 \text{ GeV})\lambda^2 < 0.1$ GeV.

while the remaining parameters (entering the Higgs sector at loop-level) were fixed at $M_1/M_2/M_3 = 150/300/1000$ GeV, $A_t = A_b = A_\tau = 2.5$ TeV, $M_{f_L} = M_{f_L} = 1$ TeV. The first four scan parameters are conventional, broad ranges over the probable values of μ, λ, $\tan\beta$, and A_λ. We chose the fifth parameter of the scan equal to $\mu\kappa/\lambda = \kappa s$ (where $s = \langle S\rangle$) since it is correlated with the mass of the CP-even higgs bosons as one can see in Fig. 1(left). Let us recall, that CP-even and CP-odd Higgs mass matrices ($\mathcal{M}_S$ and $\mathcal{M}_P$ respectively) can be written as follows (see e.g. [26]):

$$
\begin{aligned}
\mathcal{M}^2_{S11} &= g^2 v^2 \sin\beta^2 + \mu\cot\beta(A_\lambda + \kappa s) \\
\mathcal{M}^2_{S22} &= g^2 v^2 \cos\beta^2 + \mu\tan\beta(A_\lambda + \kappa s) \\
\mathcal{M}^2_{S33} &= \lambda A_\lambda \frac{v^2\sin 2\beta}{2s} + \kappa s(A_\kappa + 4\kappa s) \\
\mathcal{M}^2_{S12} &= (\lambda^2 - g^2/2)v^2\sin 2\beta - \lambda s(A_\lambda + \kappa s) \\
\mathcal{M}^2_{S13} &= \lambda v(2\lambda s\sin\beta - \cos\beta(A_\lambda + 2\kappa s)) \\
\mathcal{M}^2_{S23} &= \lambda v(2\lambda s\cos\beta - \sin\beta(A_\lambda + 2\kappa s))
\end{aligned} \tag{3}
$$

$$
\begin{aligned}
\mathcal{M}^2_{P11} &= \frac{2\lambda s}{\sin 2\beta}(A_\lambda + \kappa s) \\
\mathcal{M}^2_{P22} &= 2\lambda\kappa v^2\sin 2\beta + \lambda A_\lambda\frac{v^2\sin 2\beta}{2s} - 3\kappa A_\kappa s \\
\mathcal{M}^2_{P12} &= \lambda v(A_\lambda - 2\kappa s)
\end{aligned} \tag{4}
$$

Generally, a_1 is light if the parameters of the model are near Peccei-Quinn (PQ) symmetry limit ($\kappa{\to}0$) or/and near the R-symmetry (RS) limit ($A_\kappa, A_\lambda{\to}0$). One can see from Eq.(4), that a_1 becomes a massless axion in both limits and can be decomposed in terms of weak eigenstates H_{uI}, H_{dI} and S_I as (see e.g. [35]):

$$a_1 = c_{\theta_P} A + s_{\theta_P} S_I \tag{5}$$

where $A = \cos\beta H_{uI} + \sin\beta H_{dI}$. In the case of PQ limit mixing parameters $c_{\theta P}$, $s_{\theta P}$ are:

$$c_{\theta_P} = \frac{v\sin 2\beta}{\sqrt{v^2\sin^2 2\beta + 4s^2}}, s_{\theta_P} = -\frac{2s}{\sqrt{v^2\sin^2 2\beta + 4s^2}}. \tag{6}$$

In the case of RS limit, the same parameters are:

$$c_{\theta_P} = \frac{v\sin 2\beta}{\sqrt{v^2\sin^2 2\beta + s^2}}, s_{\theta_P} = \frac{s}{\sqrt{v^2\sin^2 2\beta + s^2}}. \tag{7}$$

For small λ, A_λ and A_κ, the $\mathcal{M}^2_{S33}$ determines the mass of the lightest CP-even Higgs mass if $\kappa s = \mu\kappa/\lambda$ is small. In this case, $m_{h1} \simeq \sqrt{4\kappa s} = 2\mu\kappa/\lambda$. This relation is illustrated in Fig. 1(left) for $\kappa\mu/\lambda < 60$ GeV when h_1
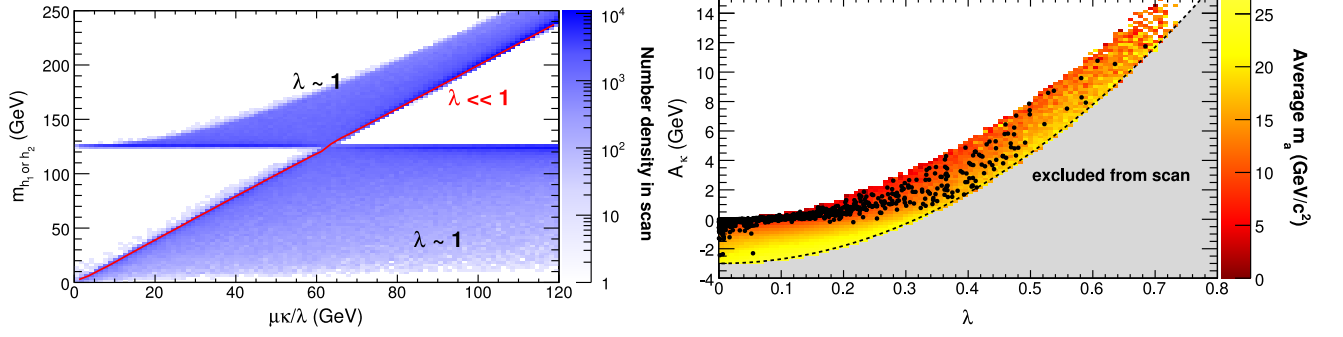
FIG. 1: Left: Lightest (h_1) and second-lightest (h_2) CP-even Higgs masses as a function of $\mu\kappa/\lambda$ and λ. The density of generated points surviving constraints is shown in the blue color scale, and the red line presents the single-valued $\lambda \ll 1$ limit. Right: mass of the CP-odd Higgs (m_a) as a function of A_κ and λ. The color scale is the average mass in each bin, and filled circles are models with $m_a < 2m_\tau$. Low m_a region follows the parabolic curve, $A_\kappa - (30 \text{ GeV})\lambda^2 \geq 0$.

with $m_{h1} < 120$ GeV has a significant singlet component, especially for small values of λ (and A_λ) when the doublet-singlet mixing is suppressed. For larger values of $\kappa\mu/\lambda > 60$ GeV, $\mathcal{M}_{S33}$ starts defining the mass of the h_2 Higgs boson with mass $m_{h2} \simeq 2\kappa\mu/\lambda$ and aquires a large singlet component, while h_1 becomes essentially the SM-like Higgs. In our scan we chose the upper bound on $\kappa\mu/\lambda < 120$ GeV to create two equal size but phenomenologically distinct sub-regions.

The last parameter, $A_\kappa - (30 \text{ GeV})\lambda^2$, and its scan range is motivated by the shape of the low m_a domain shown in Fig. 1(right). In this region A_κ is limited to be small which is motivated by RS limit, pushing a_1 to be light. It selects a region with a roughly uniform distribution of light m_a between 0 and 30 GeV and removes most of the theoretically inaccessible region with $m_a^2 < 0$.

The couplings of h_1 and a, to each other and to Standard Model particles, are determined by their singlet and non-singlet componets. One should notice, that in most of the parameter space $s = \mu/\lambda \gg v\sin 2\beta$, and, therefore, as one can see from Eq.(6,7), the s_{θ_P} (which defines the signlet component of a_1) is $\simeq 1$ in both, PQ and RS limits. Indeed, we have found, that for the entire region of our interest, a_1 is close to a pure singlet (the non-singlet fraction $1 - s_{\theta_P}^2 \lesssim 10^{-4}$) but never is exactly a pure one. The singlet fraction of h_1, $\mathcal{S}_{13}^2$ is defined essentially by $\mu\kappa/\lambda$ and λ, as illustrated in Fig. 2(left). Here we denote $\mathcal{S}_{13}$ as a mixing between the first (H_{dR}) and the third (S_R) CP-even Higgs boson weak eigensttaes. Increase of λ enhances the mixing of singlet and nonsinglet Higgs boson eigenstates for both, CP-odd and CP-even Higgses.
(let us plot $\log(1 - s_{\theta_P})$ versus $\log(v\sin 2\beta\lambda/\mu)$, where v =174 GeV)

For $\mu\kappa/\lambda \lesssim 60$ GeV, h_1 is predominantly a singlet (see Fig. 2(a) leading to a strong enhancement in the h_1aa coupling due to large singlet componets of both h_1 and a_1. Figure 2(b) shows the enhancement in the

corresponding branching ratio $Br(h_1 \to a_1a_1)$ for already small values of λ. For the same reason, the h_1 coupling to SM up or down- fermions is suppressed as ilustrated in Fig. 3(a). The corresponding suppression factors are determined by the elements of CP-even Higgs mixing matrix, $\mathcal{S}_{11} = \sqrt{1 - \mathcal{S}_{13}^2 - \mathcal{S}_{12}^2}$ and $\mathcal{S}_{12} = \sqrt{1 - \mathcal{S}_{13}^2 - \mathcal{S}_{11}^2}$), respectively. **SOUNDS LIKE THE FOLLOWING IS PROBABLY NOT TRUE? One should note that h_1 coupling to W and Z-bosons can be in general somewhat less suppressed** since it is proportional to combination **TYPO IN THE FOLLOWING?** of $\mathcal{S}_{12}$ as $\mathcal{S}_{11}$ as $(\sin\beta\mathcal{S}_{12} + \cos\beta\mathcal{S}_{11})$, as illustrated in Fig. 3(b). For $\mu\kappa/\lambda \gtrsim 60$ GeV, h_1 is a SM-like Higgs with only weak couplings to a and respectively low branching ratio to a_1a_1 pairs, which can be somewhat enhanced with large values of λ softening the threshold between pure singlet and pure doublet, see Figs. 2 and 3. In Fig. 2(b) which presents branching fraction of $h_1 \to aa$ as a function of $\mu\kappa/\lambda$ for models with $m_a < 2m_\tau$ one can see that $Br(h_1 \to aa)$ remains large only when λ is large, which is related **DID YOU MEAN INCREASED SINGLET FRACTION AND LARGER COUPLING IN THE FOLLOWING?** to the increased singlet fraction of h_1 together with the increased partial decay width $\Gamma(h_1 \to aa)$. A highly-singlet h_1 simultaneously has weak coupling to Standard Model particles (for both fermions and bosons, see Fig. 3) and, as long as λ is not vanishingly small, has strong h_1aa coupling, so it decays to aa with little competition from Standard Model modes.

Because the coupling of a light nearly-singlet a to all SM particles is strongly but about equally suppressed, its branching fractions are not affected by the singlet fraction of a_1 and follow the standard mass hierarchy. Fig. 4(a) shows the the branching fraction for $a \to \mu\mu$ as obtained using NMSSMTools package. For $m_a < 2m_\tau$ the $a \to \mu\mu$ channel becomes significant, making an analysis
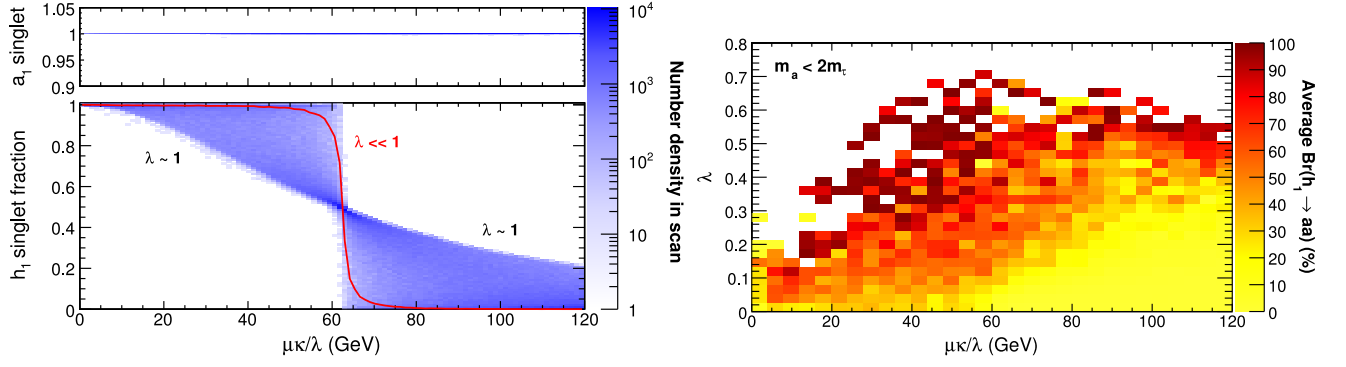
FIG. 2: Left: Singlet fraction of h_1 and a_1. The singlet fraction of a_1 is nearly constant and approximately 1.0, while the singlet fraction of h_1 depends on $\mu\kappa/\lambda$ and λ. Right: Branching fraction of $h_1 \to a_1 a_1$ in the λ, $\mu\kappa/\lambda$ plane, with the requirement that $m_a < 2m_\tau$.
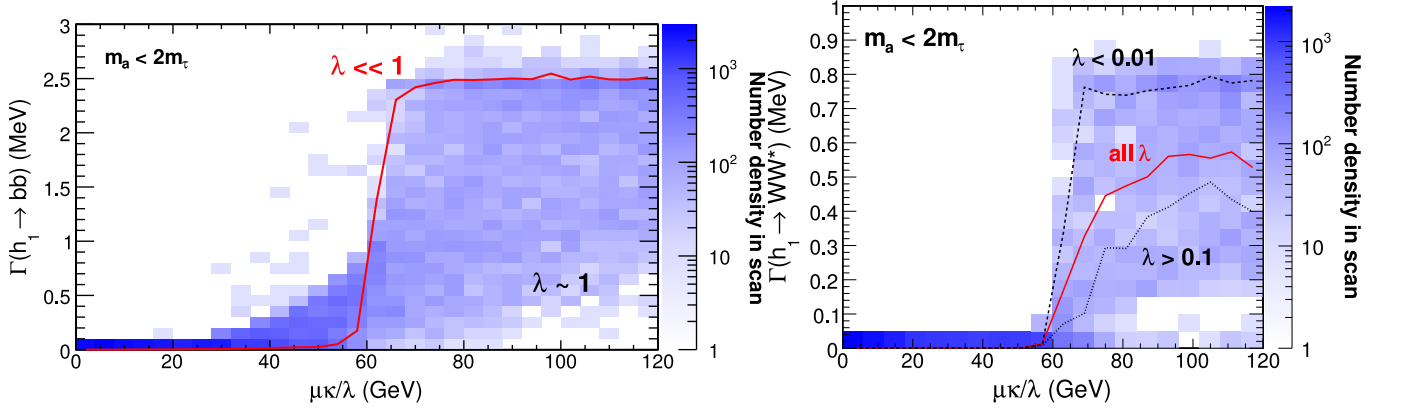

FIG. 3: Partial widths of $h_1 \to b\bar{b}$ and WW^* as a function of $\mu\kappa/\lambda$ and λ, with the requirement that $m_a < 2m_\tau$. The red line presents the single-valued $\lambda \ll 1$ limit (**the plot on the right has not been correctly updated**). **TO BE REPLACED WITH REDUCED COUPLINGS FOR DOWN-TYPE FERMIONS AND BOSONS TO HELP ILLUSTRATE OUR LATER POINT ON LEP CONSTRAINTS. IF THEY ARE DIFFERENT FOR Z AND W (I DON'T THINK SO), CHOOSE THE HZZ COUPLING**

in the four muon mode viable for experimental searches. It is important to note that the calculation shown in Fig. 4(a) was not meant tuned for $m_a < 1$ **GeV, so some corrections are necessary. First, for** $m_a < 3m_\pi$, $B(a\to\mu\mu)$ **is expected to be very high because** $q\bar{q}$ **and** gg **decays are prohibited by hadronization and spin effects need a reference and** $\gamma\gamma$ **is small (I just noticed that at m=1 GeV in the preprint with BR's we looked at, the sum of BR is ont 100%?!!!!). We compared predictions of NMSSMTools with (arXiv.0806.4411v2) and find a good agreement between the two calculations, except that the (arXiv.0806.4411v2) the** $B(\eta\to c\bar{c})$, **obtained in the context of Little Higgs model and found to be dominant above** $m_\eta =$**2.5 GeV will be strongly suppressed in the context of NMSSM (the ratio of couplings of** a_1 **to up- and down-quarks is about** $1 - 3 \times 10^{-3}$ **for the parameters space applicable to our study). NEEDS VERIFICATION: It is also worth noting that the**

recent paper by DZero has used an incorrect B - I am not sure, I will check unless someone else can check that explicitly - Alexei.

Cosmological Constraints

WMAP constraints on Cold Dark Matter (CDM) relic density can potentially be an important constraint of NMSSM parameter space under study where the CDM is lightest neutralino. To restrict our scan to models consistent with experimental measurements of relic density, we used MicrOmegas package [43] linked to NMSSMTools dark matter contribution Ω_{NMSSM} **and required** $\Omega_{NMSSM} \leq 0.1099 + 2 \times 0.0062$, **which corresponds to the 95% upper limits from the latest WMAP 5-year dataset.**

This WMAP bound excludes the region of small $\mu\kappa/\lambda$ **and** λ **as shown in Fig. 4(right) where neu-**

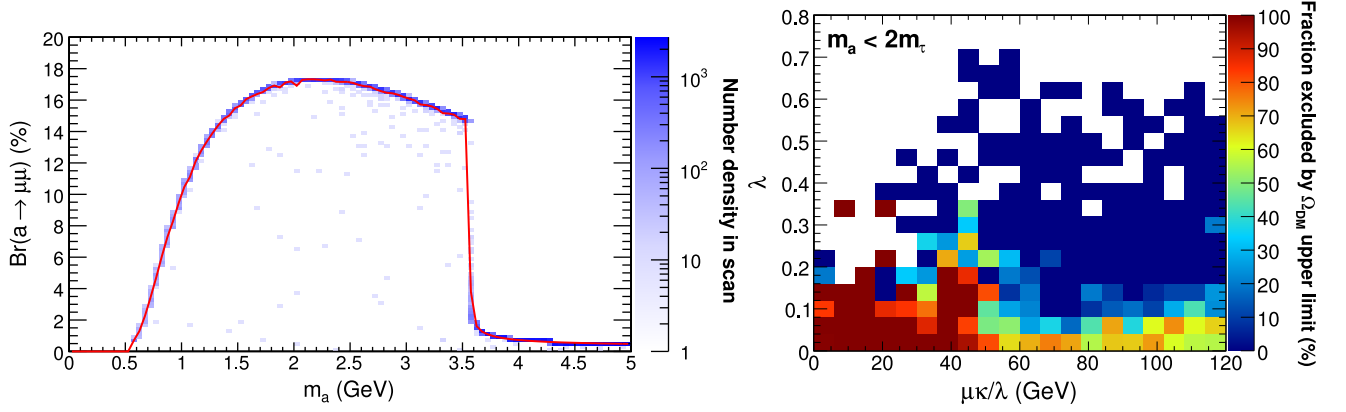FIG. 4: Left: Branching fraction of $a_1 \to \mu\mu$ for generated models as a function of m_a. The red line is the average as a function of m_a, demonstrating that the branching fraction is nearly a strict function of mass. The threshold at 3.55 GeV is $2m_\tau$. **ADD SHADED RECTANGULAR TO COVER THE REGION BELOW 0.5 SAYING THAT a WILL HAVE LARGE BR TO MUONS IN THAT REGION AND REFER TO TEXT. WE ALSO NEED TO SAY THAT THE PAPER CITED BY D0 GIVES 27% BR FOR MUONS. NEED SASHA TO LOOK INTO THIS. ALSO, WE ARE NOT GENERATING ANY POINTS BELOW 0.5 GEV B/C WE DID NOT TRY HARD ENOUGH. WE SHOULD BE ABLE TO GET THOSE BY CONSTRAINING THE SIXTH REQUIREMENT TO BE VERY SMALL NEGATIVE NUMBER. IT DOES NOT MEAN THAT NMSSMTOOLS WILL CORRECTLY CALCULATE BR RATIO THERE, BUT IT IS AN INTERESTING REGION, ISN'T IT?** Right: fraction of models with $m_a < 2m_\tau$ excluded by the WMAP dark matter constraint as a function of λ and $\mu\kappa/\lambda$. **SECOND PLOT IS A CANDIDATE TO GO**

tralino is being driven to be light and weakly interacting to SM particles which suppress neutralino annihilation rate and respectively enhances neutralino relic density to unacceptably large values.

Figure 5(a&b) show the density of models generated and those surviving WMAP constraints as a function of λ and $\mu\kappa/\lambda$.

Constraints from Direct Searches at Colliders

Figure 5-c shows the density of models surviving both WMAP and LEP constraints. LEP measurements exclude $h_1 \to aa$ within the kinematic limits of $e^+e^- \to Zh_1$, $45 < m_{h_1} < 86$ GeV, and the detector efficiency for light CP-odd Higgs bosons, $m_a > 2$ GeV [ref]. Figure 5 presents these experimental limits. (Need more discussion here, will do later).

In addition to LEP data, there have been several recent attempts aimed at direct searches. Searches at lower energy e^+e^- colliders [40, 41] have been focusing on searching for the CP-odd Higgs via $\Upsilon \to \gamma a_1$ followed by a_1 decay to leptons. Neither of these searches can lead to any constraints on the NMSSM models with low m_a because a_1 is always heavily dominated by singlet component (see the top plot in **Fig. 2**) and has absolutely negligible bba_1 coupling. (Is it sufficiently generic statement or is there smth specific in what

we do other that asking for low m_a that makes a_1 a singlet?). Did CLEO even look for such light mA? I thought they we looking for taus. Our observations are confirmed by the results obtained with the newest version of NMSSMTools.

Another recent paper by $D\emptyset$ [42] describes the search for $a_1 a_1 \to \mu\mu\mu\mu$ using Tevatron data. To interpret the $D\emptyset$ result, we calculate the NLO production cross-section for $p\bar{p} \to h_1$ in NMSSM using the SM NLO calculations for $gg \to H_{SM}$ [36] and $b\bar{b} \to H_{SM}$ with QCD-improved (running) Yukawa couplings [38] corrected for differences in coupling between SM and NMSSM using the NMSSM-Tools:

$$\sigma(gg \to h_1) = \sigma(gg \to H_{SM})\frac{\Gamma(h_1 \to gg)}{\Gamma(H_{SM} \to gg)} \quad (8)$$

$$= \sigma(gg \to H_{SM})\frac{Br(h_1 \to gg)\Gamma^{tot}(h_1)}{\Gamma(H_{SM} \to gg)}$$

$$\sigma(b\bar{b} \to h_1) = \sigma(b\bar{b} \to H_{SM})\left(\frac{Y_{bbh_1}}{Y_{bbH_{SM}}}\right)^2 \quad (9)$$

where $\sigma(gg \to H_{SM})$ and $\Gamma(H_{SM} \to gg)$ is calculated using HIGLU, while $Br(h_1 \to gg)$, $\Gamma^{tot}(h_1)$, and the ratio of Yukawa couplings $Y_{bbh_1}/Y_{bbH_{SM}}$ are obtained using NMSSMTools.

We select models for which $\sigma(p\bar{p} \to h_1) \times B_{h_1 \to aa \to 4\mu}$ does not exceed the upper limit of $\sigma_{95\%} = 6$ fb obtained in [42]. **BECAUSE PUBLISHED LIMIT MUST BE A FUNCTION OF h1 MASS, WE CORRECT $\sigma_{95\%}$ BY SCALING**
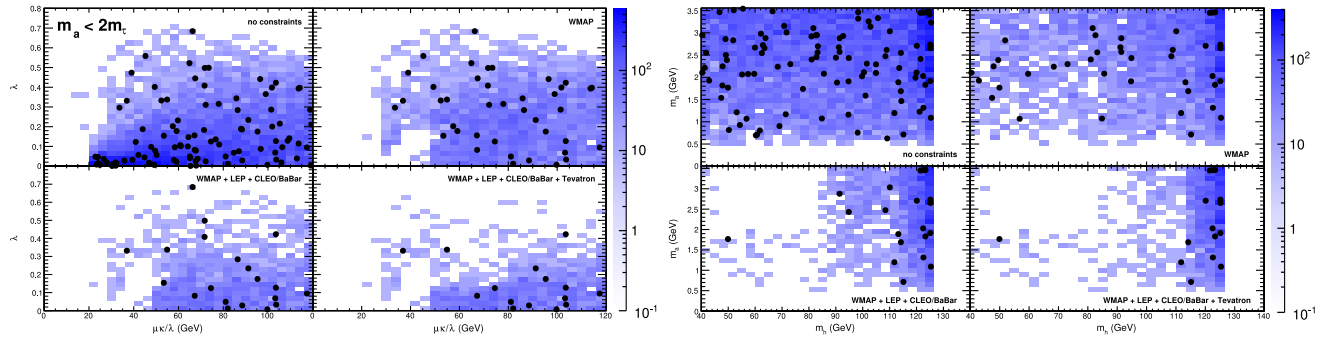
FIG. 5: Sampled points with $m_a < 2m_\tau$ and experimental constraints successively applied. Left: λ vs. $\mu\kappa/\lambda$, right: m_a vs. m_h. Color scale is number density and filled points are 100 models (before application of experimental constraints).

IT WITH $\alpha(m_{h1})/\alpha_0$, **WHERE** α_0 **is the acceptance given in [42] for mass** $m_{h1} = XXX$ **and** $\alpha(m_{h1}) = (m_{h1}/XXX) \times \alpha_0$ **Sasha: let use different name for** α**, it triggers** α_S **etc.. Figure 5 shows the density of low** m_a **models surviving WMAP, LEP and Tevatron constraints. It turns out that for** $\mu\kappa/\lambda < 60$ **(non-SM** h_1 **lighter than 120 GeV), the cross-section is strongly suppressed even compared to SM for low** m_a **because** h_1 **has a large singlet fraction. For larger** $\mu\kappa/\lambda$ **the lighest CP-even higgs** h_1 **becomes the SM-like Higgs and has negligible** $h_1 \to aa$ **branching. These effects lead to the Tevatron data having only a very small impact on the allowed NMSSM parameter space. A significant improvement in Tevatron reach for NMSSM would have required a large increase in integrated luminosity likely leaving it up to LHC to make a definitive discovery or exclusion of NMSSM models with low** m_a**.**

Summary

Existing data provides only partial constraints. Requirement of the model consistency with cosmoogical data leads to XXX. Tevatron data allows constraining of the surviving fraction of the paramater space, but only weakly. Further exploration of this region cannot be done at Tevatron b/c that would require a very significant increase in the size of the datasets. Conclusive exclusion or discovery of new physics in this scenario would require a dedicated analysis performed at LHC. In the following, we describe such analysis and discuss its sensitivity.

DEDICATED SEARCH FOR NMSSM AT LHC

The main characteristic of the signal is two back-to-back di-muon pairs with pair consisting of spatially close muons. The di-muon pairs should have invariant masses consistent with each other, which also allows a direct measurement of m_a**. Additionally, the four muon invariant mass distribution should have a narrow spike corresponding to the** m_h **mass. We use these striking features of signal events in designing the analysis suitable for early LHC running.**

The four muon final state considered in this analysis is experimentally a very clean signature with relatively low backgrounds. Therefore, instead of using the Vector Boson Fusion (VBF) chosen in earlier NMSSM searches targeting the $m_a > 2m_\tau$ **region, we focus on the largest Higgs production modes at the LHC,** $gg \to h_1$ **and** $b\bar{b} \to h_1$**. To calculate NMSSM NLO cross-section for** $pp \to h_1$ **we follow the same procedure (Eqs. 9 and 9) as for the Tevatron case based on rescaling NLO calculations [36, 38] to correct for differences in couplings between SM and NMSSM. Similar to the Tevatron case, the cross-section is strongly suppressed compared to SM if** h_1 **has a large singlet fraction. Figure 6 shows the production cross-section for 14 TeV** $pp \to h_1 X$ **as a function of** $\mu\kappa/\lambda$**. Note that the low** $\mu\kappa/\lambda$ **and low** λ **region is excluded by WMAP, see Fig. 5. The non-excluded region have appreciable production cross-section.**

Analysis Selections

We use Pythia to generate signal event templates with m_h **in the range from 70 to 140 GeV/c^2 and** m_a **in the range from 0.5 to 4 GeV/c^2). For detector response emulation, we chose the CMS detector as a benchmark and used its parameters descibed in CMS Technical Design Report. The key parameters important for this analysis are muon momentum resolution, low threshold on muons to reach the muon system, acceptance**

and average muon reconstruction efficiencies.

The analysis starts by requiring at least four muon candidates with $p_T > 5$ GeV/c in the fiducial volume of the detector $|\eta| < 2.4$, of which at least one has to have $p_T > 20$ GeV/c to suppress major backgrounds and to satisfy trigger requirements. Each event must have at least two muon candidates of positive and negative charge each. For surviving events, we define quadruplets of candidates consisting of two positive and two negatively charged muon candidates. Next, we sort the four muon candidates in quadruplet into two di-muon pairs by minimizing the quantity $(\Delta R(\mu_i, \mu_j)^2 + \Delta R(\mu_k, \mu_l)^2)$ under the constarint that each di-muon pair consists of two muon candidates of opposite charge. Quadruplets in which ΔR between muons in any of the two pair exceeds 0.5 are discarded as inconsistent with signal topology. Acceptance of the selections listed above is shown in Fig. 7 for several representative choices of values for m_h and m_a.

Requirement of four sufficiently energetic muons in the event drastically reduces contributions of potential backgrounds for this analysis. After acceptance selections, the dominant background is due to QCD multijet production where muons originate from either heavy flavor quark decays or from K/π decays in flight. We use Pythia to estimate the QCD multijet background and we estimate it at this stage to be approximately 2.6 events/pb^{-1} (approximately half due to true muons and the rest from events with both prompt muons and muons from decays in flight). We also considered electroweak backgrounds estimated using CompHEP $pp \to 4l + X$ process to be 0.04 events/pb^{-1} and direct J/psi production (Pythia), which was found to be completely negligible. Other SM backgrounds (top, W+jets) are negligible in the region of interest of this analysis.

The backgrounds are further reduced by applying kinematics requirements consistent with the expected signal siganture. We calculate invariant mass of each of the di-muon pair, m_{12} and m_{34}, as well as the invariant mass of all four muons denoted as M. Figure 8a) shows the invariant mass of the muon pairs passing all selections in signal events for two choices of m_h and m_a. Figure 8b) shows the distribution of the invariant mass M of the four muon system for two benchmark points. To focus on the region of interest, we require $M > 60$ GeV/c^2, $m_{12} < 4$, $m_{34} < 4$, which reduces QCD background to 0.4 events/pb^{-1}.

To ensure the compatibility of the measured invariant masses of two di-muon pairs, one could apply a simple cut $|m_{12} - m_{34}| < 0.08 + 0.005 * (m_{12} + m_{34})$. This cut would enforce the requirement that the two pair masses are consistent with each other and it takes into account widening of the absolute resolution in the reconstructed di-muon mass as a function of mass. If applied, the only background that still may be not completely negligible is QCD multi-jet, for which we conservatively estimate the upper bound to be 0.02 events/pb^{-1}. However, instead of applying this selection explicitly, a better approach would be to fit the data in the 3D space of measured values of $(m_{12}, m_{34}, m_{1234})$ taking into account kinematical properties of signal events. This approach allows maximizing signal acceptance and therefore statistical power of the analysis. It is also convenient from experimental point of view as the backgrounds will be distributed in some smooth fashion over the 3D space allowing fitting the 3D distribution to estimate backgrounds directly from the data. Potential signal would appear as a concentration of events in one specific region in the 3D space (a 3D "bump"). We use a binned likelihood defined as a function of parameters m_a, m_h and effective signal cross section $\sigma \times B(h \to aa)B^2(a \to \mu\mu)$. Thus defined likelihood is used to fit pseudodata generated using either background or signal+background templates. We estimate sensitivity of the proposed analysis and present it in terms of the 95% C.L. exclusion levels for signal cross-section using Bayesian technique.

If necessary, further large background suppression can be obtained by adding the isolation requirement to one or both di-muon pairs in the event, e.g. by setting the upper bound on the sum of transverse momenta of all tracks in a cone around the reconstructed direction of the di-muon pair excluding momenta of the two muon tracks. Such requirement can allow a very substantial suppression of the dominant source of the background coming from events with one or more muons originating from jets. We choose not to use this critirea as our estimates show that the final rate of such background events is already very low. If data shows larger contribution of these events, this isolation requirement would allow bringing backgrounds back to very low level at a moderate cost to signal acceptance.

Results

We calculate the 95% C.L. upper limit on the product $\sigma(pp \to h)B_{h \to aa}B^2_{a \to \mu\mu}\alpha$, using Bayesian technique which is 0.0293 pb at $L = 100$ pb^{-1}, approximately 3 events. In vast majority of pseudo-experiments, this limit is independent of m_h and
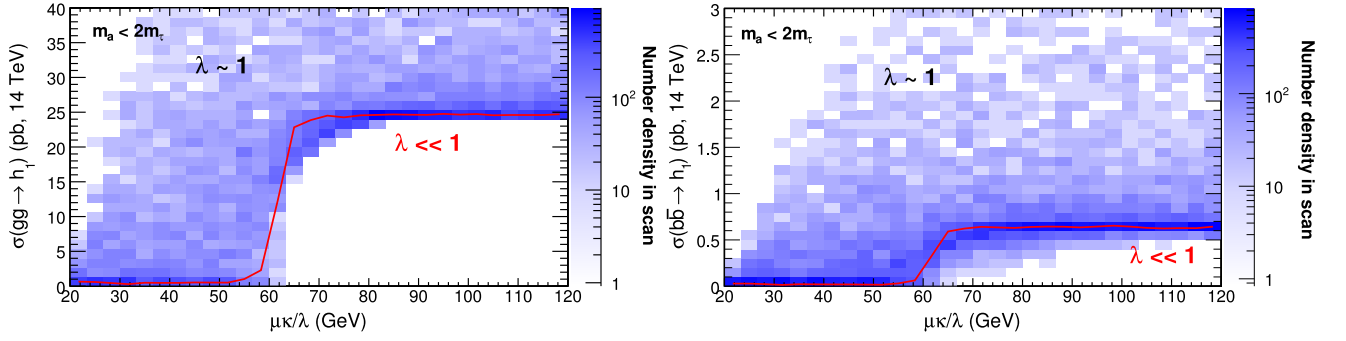
FIG. 6: 14 TeV production cross-section of h_1 as a function of $\mu\kappa/\lambda$ and λ, from gg (left) and $b\bar{b}$ (right), with the requirement that $m_a < 2m_\tau$. The red line represents the single-valued $\lambda \ll 1$ limit.
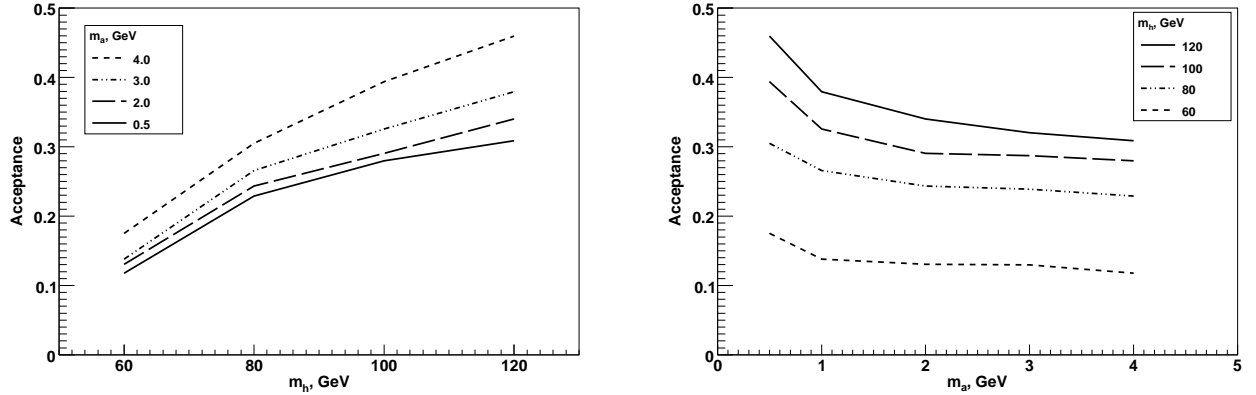

FIG. 7: Acceptance as a function of m_a for fixed m_h. Acceptance as a function of m_h for fixed m_a.

TABLE I: Expected number of background events per 100 pb^{-1} of luminosity after selection cuts.

Selections	4 leptons	QCD multi-jet
$p_T(\mu_1) > 20$ GeV/c& $p_T(\mu_i) > 5$ GeV/c i=2,3,4	4.8 ± 0.2	267 ± 23
$m_{12}, m_{34} < 4$ GeV/c^2	0.024 ± 0.012	90 ± 13
$m_{1234} > 60$ GeV/c^2	0.010 ± 0.007	39 ± 9
$\|m_{12} - m_{34}\| < 0.08$ GeV $+0.005 * (m_{12} + m_{34})$	$0.000^{+0.005}_{-0.000}$	$0.00^{+1.95}_{-0.00}$

TABLE II: 95% C.L. upper limit on $\sigma(pp\rightarrow h)B_{h\rightarrow aa}$ (pb) at $L = 100$ pb^{-1} at the LHC. Variations in $\sigma_{95\%}$ as a function of m_a driven by dependency of $B_{a\rightarrow\mu\mu}$ on m_a, while tightening of the limit towards higher m_h is due to increase in acceptance with m_h. **We need to add a second set of numbers for 1 ifb, but if backgrounds are too big we need to add isolation or at least some educated guess on how isolation will affect backgrounds and signal.**

m_h, m_a (GeV)	0.5	1.0	2.0	3.0	4.0
80	∞	10.9	4.1	4.6	2400
100	∞	8.9	3.4	3.8	2000
120	∞	7.7	2.9	3.4	1800

m_a because the effective signal region that dominates signal significance in the fitter is essentially background free and probability to observe any pseudodata event is very small. The upper limit on $\sigma(pp\rightarrow h)B_{h\rightarrow aa}$ is shown as a function of m_h and m_a in Table II. Note that $B_{h\rightarrow aa}$ is close to 100% in much of the selected region of NMSSM parameter space.
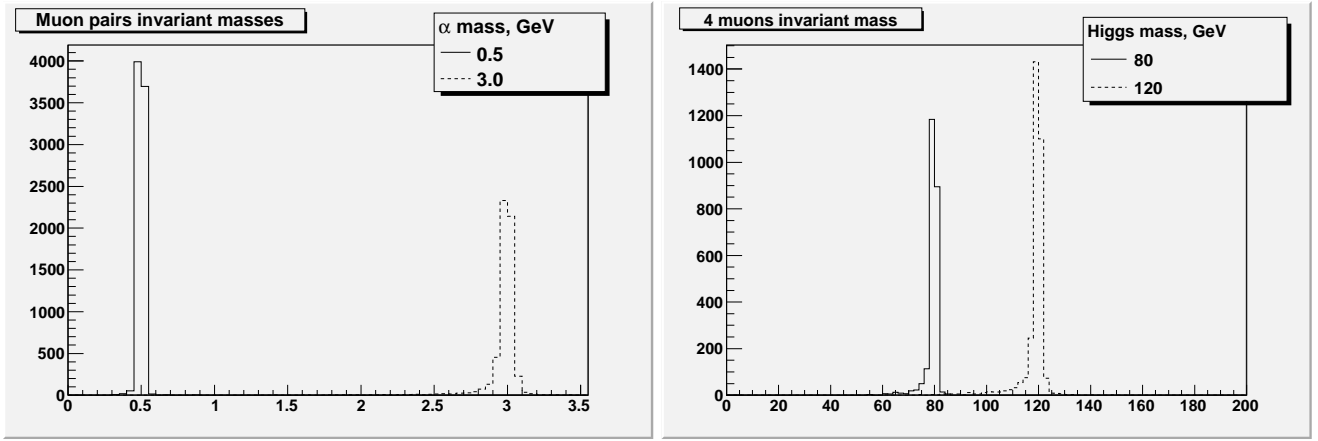
RESULTS

TO BE WRITTEN

FIG. 8: Left: Reconstructed invariant mass of reconstructed muon pairs for $m_a = 0.5$ and 3 GeV/c^2 (in both cases $m_H = 100$ GeV/c^2). Right: Reconstructed invariant of four muons for $m_H = 80$ and $m_H = 120$ GeV/c^2 (in both cases $m_a = 3.0$ GeV).
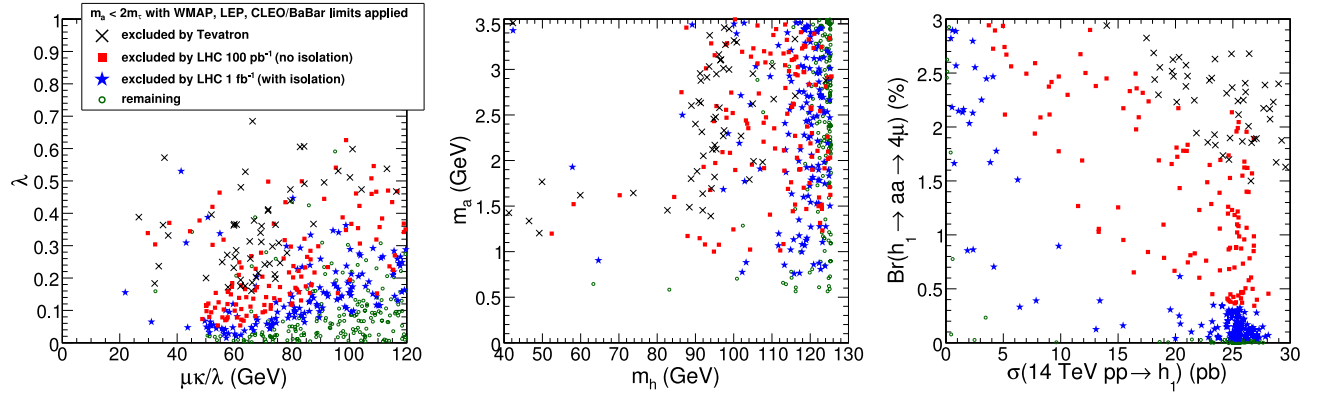

FIG. 9: Sampled models excluded by the Tevatron and LHC (with $m_a < 2m_\tau$, WMAP, and LEP constraints applied in all cases). With only 100 pb^{-1}, the LHC's reach extends beyond that of the Tevatron.

[1] H. P. Nilles, M. Srednicki and D. Wyler, Phys. Lett. B 120 (1983) 346.
[2] J. M. Frere, D. R. T. Jones and S. Raby, Nucl. Phys. B 222 (1983) 11.
[3] J. R. Ellis, J. F. Gunion, H. E. Haber, L. Roszkowski and F. Zwirner, Phys. Rev. D 39 (1989) 844.
[4] M. Drees, Int. J. Mod. Phys. A 4 (1989) 3635.
[5] U. Ellwanger, Phys. Lett. B 303 (1993) 271 [arXiv:hep-ph/9302224].
[6] U. Ellwanger, M. Rausch de Traubenberg and C. A. Savoy, Phys. Lett. B 315 (1993) 331 [arXiv:hep-ph/9307322].
[7] T. Elliott, S. F. King and P. L. White, Phys. Rev. D 49 2435 (1994) 2435 [arXiv:hep-ph/9308309].
[8] P. N. Pandita, Z. Phys. C 59 (1993) 575.
[9] U. Ellwanger, M. Rausch de Traubenberg and C. A. Savoy, Z. Phys. C 67 (1995) 665 [arXiv:hep-ph/9502206].
[10] S. F. King and P. L. White, Phys. Rev. D 52 (1995) 4183 [arXiv:hep-ph/9505326].
[11] F. Franke and H. Fraas, Int. J. Mod. Phys. A 12 (1997) 479 [arXiv:hep-ph/9512366].
[12] U. Ellwanger, M. Rausch de Traubenberg and C. A. Savoy, Nucl. Phys. B 492 (1997) 21 [arXiv:hep-ph/9611251].
[13] D. J. Miller, R. Nevzorov and P. M. Zerwas, Nucl. Phys. B 681 (2004) 3.
[14] J. E. Kim and H. P. Nilles, Phys. Lett. B 138, 150 (1984).
[15] R. Dermisek and J. F. Gunion, Phys. Rev. Lett. 95, 041801 (2005) [arXiv:hep-ph/0502105].
[16] B. A. Dobrescu, G. L. Landsberg and K. T. Matchev, Phys. Rev. D 63, 075003 (2001) [arXiv:hep-ph/0005308]; B. A. Dobrescu and K. T. Matchev, JHEP 0009, 031 (2000)

[arXiv:hep-ph/0008192].

[17] J. F. Gunion, H. E. Haber and T. Moroi, *In the Proceedings of 1996 DPF / DPB Summer Study on New Directions for High-Energy Physics (Snowmass 96), Snowmass, Colorado, 25 Jun - 12 Jul 1996, pp LTH095* [arXiv:hep-ph/9610337]; U. Ellwanger, J. F. Gunion and C. Hugonie, arXiv:hep-ph/0111179

[18] J. R. Ellis, J. F. Gunion, H. E. Haber, L. Roszkowski and F. Zwirner, Phys. Rev. D 39, 844 (1989); B. A. Dobrescu, G. L. Landsberg and K. T. Matchev, Phys. Rev. D 63, 075003 (2001) [arXiv:hep-ph/0005308];
U. Ellwanger, J. F. Gunion, C. Hugonie and S. Moretti, arXiv:hep-ph/0305109; U. Ellwanger, J. F. Gunion, C. Hugonie and S. Moretti, arXiv:hep-ph/0401228; U. Ellwanger, J. F. Gunion and C. Hugonie, JHEP 0507, 041 (2005) [arXiv:hep-ph/0503203].

[19] S. Moretti, S. Munir and P. Poulose, Phys. Lett. B 644, 241 (2007) [arXiv:hep-ph/0608233];

[20] S. Chang, P. J. Fox and N. Weiner, Phys. Rev. Lett. 98, 111802 (2007) [arXiv:hep-ph/0608310].

[21] R. Dermisek and J. F. Gunion, Phys. Rev. D 75, 075019 (2007) [arXiv:hep-ph/0611142].

[22] K. Cheung, J. Song and Q. S. Yan, Phys. Rev. Lett. 99, 031801 (2007) [arXiv:hep-ph/0703149].

[23] J. R. Forshaw, J. F. Gunion, L. Hodgkinson, A. Papaefstathiou and A. D. Pilkington, JHEP 0804 (2008) 090 [arXiv:0712.3510 [hep-ph]].

[24] A. Belyaev, S. Hesselbach, S. Lehti, S. Moretti, A. Nikitenko and C. H. Shepherd-Themistocleous, arXiv:0805.3505 [hep-ph].

[25] A. Menon, D. E. Morrissey and C. E. M. Wagner, Phys. Rev. D 70 (2004) 035005 [arXiv:hep-ph/0404184]; D. G. Cerdeno, C. Hugonie, D. E. Lopez-Fogliani, C. Munoz and A. M. Teixeira, JHEP 0412 (2004) 048 [arXiv:hep-ph/0408102]; G. Belanger, F. Boudjema, C. Hugonie, A. Pukhov and A. Semenov, JCAP 0509, 001 (2005) [arXiv:hep-ph/0505142]; J. F. Gunion, D. Hooper and B. McElrath, Phys. Rev. D 73, 015011 (2006) [arXiv:hep-ph/0509024]; F. Ferrer, L. M. Krauss and S. Profumo, Phys. Rev. D 74, 115007 (2006) [arXiv:hep-ph/0609257]; D. G. Cerdeno, E. Gabrielli, D. E. Lopez-Fogliani, C. Munoz and A. M. Teixeira, JCAP 0706, 008 (2007) [arXiv:hep-ph/0701271]; C. Hugonie, G. Belanger and A. Pukhov, JCAP 0711, 009 (2007) [arXiv:0707.0628 [hep-ph]]; V. Barger, P. Langacker, I. Lewis, M. McCaskey, G. Shaughnessy and B. Yencho, Phys. Rev. D 75, 115002 (2007) [arXiv:hep-ph/0702036]. S. Kraml, A. R. Raklev and M. J. White, Phys. Lett. B 672, 361 (2009) [arXiv:0811.0011 [hep-ph]]; G. Belanger, C. Hugonie and A. Pukhov, JCAP 0901, 023 (2009) [arXiv:0811.3224 [hep-ph]].

[26] U. Ellwanger, J.F. Gunion and C. Hugoine, JHEP 0502, 066 (2005).

[27] U. Ellwanger, C. Hugoine, Comput. Phys. Commun. 175, 290 (2006).

[28] F. Domingo and U. Ellwanger, arXiv:0710.3714 [hep-ph].

[29] D. N. Spergel *et al.* [WMAP Collaboration], As-

TABLE III: Background samples normalization

Sample	σ	N_{evt}^{gen}	Filter efficiency	L_{eff}	$f = L_{100}/L$
$\mu + x$	$0.5091mb$	6238383	0.000239	$51.2709pb^{-1}$	1.9504
4 leptons	$0.538pb$	10995	1.0	$20436.803pb^{-1}$	0.0049
J/ψ	$0.127.2nb$	1413803	0.0074	$1502.00pb^{-1}$	0.0666

trophys. J. Suppl. 148, 175 (2003) [arXiv:astro-ph/0302209]; C. L. Bennett *et al.* [WMAP Collaboration], Astrophys. J. Suppl. 148, 1 (2003) [arXiv:astro-ph/0302207]; D. N. Spergel *et al.* [WMAP Collaboration], Astrophys. J. Suppl. 170, 377 (2007) [arXiv:astro-ph/0603449].

[30] V. M. Abazov *et al.* [D0 Collaboration], Phys. Rev. Lett. 103, 061801 (2009) [arXiv:0905.3381 [hep-ex]].

[31] G. Abbiendi *et al.* (OPAL Collaboration), Eur. Phys. J. C 18, 425-445 (2001).

[32] G. Abbiendi *et al.* (OPAL Collaboration), Eur. Phys. J. C 27, 483-495 (2003), arXiv:0209068v1 [hep-ex].

[33] W. Love *et al.* [CLEO Collaboration], Phys. Rev. Lett. 101, 151802 (2008) [arXiv:0807.1427 [hep-ex]].

[34] B. Aubert *et al.* [BABAR Collaboration], Phys. Rev. Lett. 103, 081803 (2009) [arXiv:0905.4539 [hep-ex]].

[35] U. Ellwanger, C. Hugonie and A. M. Teixeira, arXiv:0910.1785 [hep-ph].

[36] M. Spira, A. Djouadi, D. Graudenz and P. M. Zerwas, Nucl. Phys. B 453, 17 (1995) [arXiv:hep-ph/9504378].

[37] A. Djouadi, J. Kalinowski and M. Spira, Comput. Phys. Commun. 108, 56 (1998) [arXiv:hep-ph/9704448].

[38] C. Balazs, H. J. He and C. P. Yuan, Phys. Rev. D 60, 114001 (1999) [arXiv:hep-ph/9812263].

[39] A. Belyaev, J. Pumplin, W. K. Tung and C. P. Yuan, JHEP 0601, 069 (2006) [arXiv:hep-ph/0508222].

[40] (CLEO Collaboration) Phys. Rev. D 76, 117102 (2007);

[41] (BaBar) Phys. Rev. Lett. 103:081803 (2009);

[42] PRL 103, 061801 (2009).

[43] G. Belanger, F. Boudjema, C. Hugonie, A. Pukhov, A. Semenov, JCAP 0509:001 (2005), arXiv:hep-ph/0505142

APPENDIX